Multiple *cis–trans* conformers of the prolactin receptor proline-rich motif (PRM) peptide detected by reverse-phase HPLC, CD and NMR spectroscopy

Kevin D. O'NEAL*‡‡, Mohan V. CHARI†§**, Charles H. McDONALD††, Richard G. COOK‡††, Li-yuan YU-LEE‡§‖, Joel D. MORRISETT§¶**‡‡ and William T. SHEARER*‡,‡‡,§§

Departments of *Pediatrics, Allergy and Immunology Section, †Radiology, ‡Microbiology and Immunology, §Medicine, ‖Cell Biology, and ¶Biochemistry, **NMR Spectroscopy Laboratory, and ††Advanced Technologies Laboratories, Baylor College of Medicine, Houston, TX 77030, U.S.A.

An eight-amino-acid synthetic peptide (Ile[1]-Phe[2]-Pro[3]-Pro[4]-Val[5]-Pro[6]-Gly[7]-Pro[8]) corresponding to the conserved proline-rich motif (PRM) of the intracellular domain of the prolactin receptor (PRL-R) was studied by one- and two-dimensional (1D and 2D) proton NMR spectroscopy in water and DMSO in order to characterize its conformational dynamics. The purified PRL-R PRM peptide eluted as two partially resolved peaks in equilibrium on reverse-phase HPLC (RP-HPLC) at 20 °C with a ratio of 60:40. At 30 °C, the two peaks coalesced into a single peak. The two RP-HPLC peaks correspond to two peptide conformers resulting from the slow *cis–trans* isomerization of one of the four proline amide bonds. Although the peptide has only three amide (NH) protons, its 1D NMR spectrum in water contains approximately 15 discernible NH region peaks, providing evidence for multiple conformers. The amide resonances were assigned on the basis of 2D-COSY spectra, chemical shift values, resonance splitting patterns and temperature coefficients. The *cis*:*trans* ratio for each proline in water, calculated from integrated intensities and/or peak heights of the appropriate resonances, were Phe[2]-Pro[3] (35:65), Pro[3]-Pro[4] (40:60), Val[5]-Pro[6] (70:30), and Gly[7]-Pro[8] (30:70). Temperature studies (25–70 °C) were used to semi-quantitatively estimate the rates of isomerization for the different prolines. In water, Pro[8] undergoes rapid isomerization; Pro[3] isomerizes at an intermediate rate; while Pro[4] and Pro[6] both appear to isomerize very slowly since no coalescence of amide resonances was observed. In DMSO, only Pro[4] displayed slow isomerization. Slow kinetics combined with a similar 60:40 ratio of conformers determined by RP-HPLC and NMR suggests that isomerization of the Pro[3]-Pro[4] bond generates the two RP-HPLC peaks. Both proximal and distal proline isomerization effects were observed in NMR experiments. All of the 16 theoretical ($2^4 = 16$) proline configurations appear to exist in equilibrium in water. The predominant (19%) conformation, *trans*[3]-*trans*[4]-*cis*[6]-*trans*[8], may reflect the configuration of the PRM prolines in the native PRL-R. Isomerization of Pro[6] from *cis* to *trans* generates an interaction between the peptide N-and C-termini, suggesting an overall pseudo-cyclic conformation. This all-*trans* proline configuration may play an important biochemical role in the function of cytokine/haematopoietin receptors. A model is proposed which suggests that isomerization of the PRM by an immunophilin such as the FK506-binding protein (FKBP) serves as an on–off switch for cytokine receptor activation.

INTRODUCTION

The prolactin receptor (PRL-R) is a member of the cytokine/haematopoietin receptor superfamily. This large superfamily of receptors is defined by three conserved structural motifs, including two pairs of Cys residues and the Trp-Ser-Xaa-Trp-Ser (WSXWS, single-letter code, where X is any amino acid) motif in the extracellular domain [1], and the proline-rich motif (PRM) in the cytoplasmic domain [2]. The PRM is an eight-amino-acid motif found in the membrane proximal region of the cytoplasmic domain of all cytokine receptors, and which overlaps with box 1 [3]. The receptors for PRL and other cytokines signal through the rapid activation of the JAK (Janus kinase) family of receptor-associated tyrosine kinases, which subsequently phosphorylate substrate proteins including the STATs (signal transducers and activators of transcription) [4–10]. One of the earliest steps in cytokine receptor activation is subunit dimerization upon ligand binding. The PRL-R, growth hormone receptor (GH-R) and erythropoietin receptor form homodimers [11–14], while others such as the interleukin-2 receptor (IL2-R) and ciliary neurotrophic factor receptors form heteromeric complexes [15,16]. The conformational changes that occur after ligand binding and which lead to receptor oligomerization and JAK activation are not understood.

Proline is an unusual amino acid with respect to its chemistry (imide bond formation) and to its capacity to affect local polypeptide structure, where it often participates in the formation of loops, turns and the polyproline helix [17–21]. While most peptide bonds exist in the *trans* geometry, those involving proline (Xaa-Pro) occur in *cis* or *trans*. Proline isomerization, the interconversion of *cis* and *trans* conformers by 180° rotation across the imido peptide bond, is believed to be a rate-limiting step in protein folding [22]. The isomerization of proline can be catalysed by the enzyme peptidyl-prolyl isomerase (PPIase). Interestingly, the PPIases serve as the intracellular receptors for the immunosuppressive drugs cyclosporin A (CsA), FK506, and rapamycin (RAP), and are therefore also called the immunophilins [23]. The immunosuppressive drugs are thought to mimic a twisted peptidyl-prolyl bond that might occur in an endogenous peptide target. While CsA and FK506 inhibit T-cell receptor

Abbreviations used: PRL-R, prolactin receptor; PRM, proline-rich motif; 1D, one-dimensional; 2D, two-dimensional; JAK, Janus kinase; GH-R, growth hormone receptor; IL2-R, interleukin 2 receptor; PPIase, peptidyl-prolyl *cis–trans* isomerase; CsA, cyclosporin A; RAP, rapamycin; SH3, Src homology 3 domain; RP-HPLC, reverse-phase HPLC; TFA, trifluoroacetic acid; ProA, prolinamide; $\Delta\delta$, chemical shift difference; PPII, polyproline type II; FKBP12, 12 kDa FK506 binding protein.

‡‡ To whom correspondence should be addressed.

§§ To whom requests for reprints should be addressed at Texas Children's Hospital, Department of Allergy/Immunology, MC 1-3291, 6621 Fannin St., Houston, TX 77030, U.S.A.

signalling, RAP is known to inhibit the signal transduction of cytokine receptor superfamily members such as the receptors for interleukins 2, 3, 4, and 6 [24].

Most cytokine receptors contain three conserved prolines in the eight-amino acid PRM whose consensus sequence is **Al-Ar-Pro$_1$-Xaa-Al-Pro$_2$-Xaa-Pro$_3$** (where Al is an aliphatic, and Ar is an aromatic amino acid residue; for clarity, consensus residues throughout the text are in bold typeface) [2]. The PRL-R PRM Ile^{243}-Phe-Pro-Pro-Val-Pro-Gly-Pro^{250} (IFPPVPGP, single-letter code) has an additional proline in the non-conserved fourth position. The synthetic peptide used in this study is written as Ile^1-Phe^2-Pro^3-Pro^4-Val^5-Pro^6-Gly^7-Pro^8, where Pro^3 corresponds to conserved **Pro$_1$**, Pro^6 is equivalent to conserved **Pro$_2$**, and Pro^8 is analogous to **Pro$_3$**. The broad conservation of the cytoplasmic PRM in cytokine receptors suggests that it plays a critical structural and/or functional role in these proteins [2]. This idea is supported by the results of mutagenesis studies of several cytokine receptors including gp130 [3], the common β chain (β_c) for the interleukin 3, interleukin 5 and granulocyte/macrophage colony-stimulating factor receptors [25], granulocyte colony-stimulating factor receptor [26], leukaemia inhibitory factor receptor [27], IL2-Rβ [28], GH-R [29,30], Nb2 PRL-R [31] and IL5-R [32]. Studies with the three PRL-R forms (short, Nb2 and long) which differ in the distal cytoplasmic domain, indicate that the PRM is necessary but not sufficient for PRL-R signalling [33]. All three forms contain the PRM sequence, but only the Nb2 and long PRL-Rs can induce PRL-responsive genes and cellular growth in transfection studies. This suggests that C-terminal cytoplasmic sequences are also needed [33,34]. The generalization has been made that at least two prolines in the PRM are required for normal signalling to occur [35]. Of all the conserved proline residues, attention has recently focused on **Pro$_2$**. Mutation of the conserved **Pro$_2$** position in the GH-R (Pro^{284}) to Ala completely abolished the growth response, suggesting that this proline is a key residue in signal transduction [30].

The biochemical role of the PRM is not known. It may be important for folding cytokine receptors into their native structures. It may serve as a binding site for a Src homology 3 (SH3) domain, such as those found in Src tyrosine kinases and other signalling molecules [36–38]. The PRM could form an important secondary structural element required for cytokine receptor function. Alternatively, it has been suggested that the PRM may serve as an on–off switch by the isomerization of a critical proline residue that induces a conformational change in the cytoplasmic domain of the cytokine receptor [39]. Furthermore, this proline isomerization is proposed to be regulated by an immunophilin [39].

In the present study, we have used reverse-phase HPLC (RP-HPLC), circular dichroism (CD), and one- and two-dimensional (1D and 2D) proton NMR spectroscopy (^{1}H-NMR) to characterize the PRL-R PRM peptide. NMR has been used successfully to characterize *cis–trans* isomerization of prolines in several peptide and protein systems [40–44]. Characterization of the structure and conformational dynamics of the PRL-R PRM peptide, although not in the context of the entire PRL-R cytoplasmic domain, may provide insight into the structure and function of the PRM in cytokine receptors.

MATERIALS AND METHODS

Peptide synthesis

The PRL-R PRM peptide was synthesized on an Applied Biosystems (ABI) 430A peptide synthesizer (Perkin-Elmer Corp., Applied Biosystems Division, Foster City, CA, U.S.A.), using fluoren-9-ylmethoxycarbonyl (Fmoc)-protected amino acids and Rink amide 4-(2′,4′-dimethoxyphenyl-aminomethyl) phenoxymethyl (MBHA) resin (Novabiochem, La Jolla, CA, U.S.A.). The amino acids were coupled using 2-(1*H*-benzotriazol-1-yl)-1,1,3,3-tetramethyluronium hexafluorophosphate/1-hydroxybenzotriazole (HBTU/HOBT) activation and an *N*-methylpyrrolidone solvent system. The peptide was cleaved from the resin using trifluoroacetic acid (TFA)/ethanedithiol/thioanisole/phenol/water (40:1:2:2:3, by vol.) for 2 h at 20 °C, precipitated and washed three times with cold (−20 °C) diethyl ether and solubilized in HPLC-grade water. The crude product was purified using a Waters HPLC system (Millipore Corp., Milford, MA, U.S.A.) with an ABI 10 mm × 250 mm C_{18} RP-HPLC column. A 60 min gradient of 0–35 % Buffer B (100 % acetonitrile) in Buffer A (0.1 % TFA) was used.

RP-HPLC analysis

Analytical RP-HPLC of the crude PRL-R PRM peptide was performed on a Waters HPLC system using an ABI 4.6 mm × 220 mm C_8 RP-HPLC column, while preparative RP-HPLC was done using a Pharmacia 10 mm × 250 mm Sephasil C_{18} column. Temperature and rechromatography studies were carried out on a SMART® System (Pharmacia LKB Biotechnology, Uppsala, Sweden) using a 2.1 mm × 10 mm Sephasil C_{18} column. The purified PRL-R PRM peptide was characterized by amino acid analysis on an ABI 420A amino acid analyser after manual hydrolysis using a Waters Pico·Tag® work station, by N-terminal sequencing on an ABI 473A protein sequencer, and by fast-ion-bombardment MS on a ZAB-SEQ mass spectrometer (VG Instruments, Manchester, U.K.) using a liquid matrix of 1,1′-dithiodiethanol/thioglycerol (1:1, v/v) saturated with oxalic acid. The PRL-R PRM peptides with additional flanking residues, PRM4 (IFPPVPGPKIKG) and 2PRM4 (TCIFPPVPGPKIKG), were provided by Dr. Tzyy-Chyau Liang (University of Texas Health Science Center, Houston, TX, U.S.A.).

CD spectropolarimetry

Far-UV CD (260–184 nm) was carried out using a Jasco J-500A spectropolarimeter controlled by a modified version of the Jasco program CD-DP. The peptide was analysed at ∼ 1 mg/ml in water, pH 2.65, in a quartz 0.5 mm pathlength cell, using a scanning speed of 50 nm/min. Each spectrum represents 10 averaged scans from which the same number of averaged solvent scans was subtracted. The data are presented as molar ellipticity $[\theta]$ ($deg \cdot cm^2 \cdot dmol^{-1}$), which was calculated using a mean residue weight of 103. For temperature studies, the cell holder was equilibrated with an external circulating water bath and monitored using an attached Luxtron optic-fibre thermometer.

^{1}H-NMR spectroscopy

NMR analysis was done at a peptide concentration of 27 mM in $H_2O/^2H_2O$ (9:1, v/v), at pH meter reading 2.9, or in DMSO at 30 mM in 5 mm NMR tubes. The NMR spectra were acquired on a 400 MHz Bruker AM-400 wide-bore (89 mm) system operating at 9.4 T with the Aspect 3000 computer. Data processing was conducted using the Bruker software WIN-NMR (1D) and DISNMR (2D). The 1D spectra were recorded using 16×10^3 data points at 25, 30, 40, 50, 60 and 70 °C. The water signal was suppressed by presaturation for 2 s before data acquisition. The spectra were referenced against tetradeuterated sodium trimethylsilylpropionate (TSP-d_4; $\delta = 0$ p.p.m.). The 2D

data set consisted of 2×10^3 data points in the f_2 dimension with 512 increments in the f_1 dimension with zero-filling. Each f_1 spectrum was averaged over 64 or 128 transients, using a sweep width of 5000 Hz. A sinebell-squared window function was applied in both axes for processing and the data were symmetrized. Phase-sensitive COSY spectra were acquired at 25, 30, 40 and 50 °C.

RESULTS

Synthetic PRL-R PRM peptide elutes on RP-HPLC as two conformers in slow equilibrium

The covalent structure of the PRL-R PRM peptide IFPPVPGP, synthesized with a C-terminal prolinamide (ProA), is shown in Figure 1. The crude peptide chromatographed on RP-HPLC as two partially resolved peaks, which is a probable result of the slow *cis–trans* isomerization of one of the prolines. There are four Xaa-Pro (Xaa = any amino acid) peptide bonds, each of which has the potential to undergo *cis–trans* isomerization. Other possible reasons for the two peaks, including (i) presence of an impurity, (ii) charge equilibrium and (iii) aggregation, were ruled out by the persistence of the two peaks (i) after RP-HPLC purification, (ii) under pH conditions well below the pK_a of the titratable N-terminal amino group, and (iii) during a series of dilution experiments respectively (results not shown). At 25 °C, the purified peptide eluted with a peak 1/peak 2 ratio of approximately 60:40. To test the possibility that each peak represented a different proline isomer in equilibrium with the other, fractions corresponding to each peak were collected and immediately rechromatographed at 25 °C. Each peak regenerated the original two-peak pattern, indicating that the peptide is in equilibrium between two major RP-HPLC conformers (results not shown). The primary structure of the purified PRL-R PRM peptide was confirmed by amino acid analysis, peptide sequencing, and mass spectrometry which gave an m/z ratio of 822.02; the expected relative molecular mass of the PRL-R PRM is 822.99.

There are at least two properties a peptide must possess in order for it to demonstrate multiple RP-HPLC conformers at ambient temperatures. First, the structure of the conformers must be sufficiently different to cause them to interact differently with the hydrophobic adsorbing surface of the column, resulting

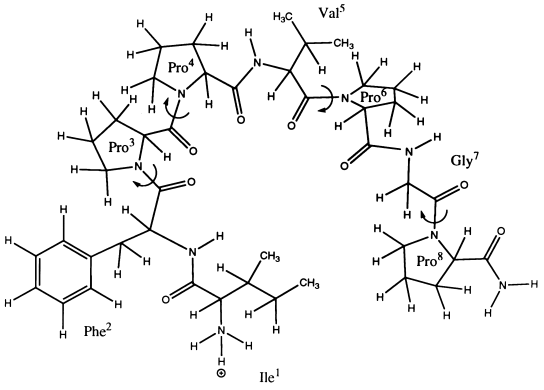

Figure 1 Covalent structure of the PRL-R PRM peptide

Each of the eight amino acids is labelled. The C-terminus contains a ProA. All protons are shown, many of which are characterized in detail by the NMR studies. Curved arrows mark the four peptide bonds containing an Xaa-Pro that may exist in either *cis* or *trans* geometry.

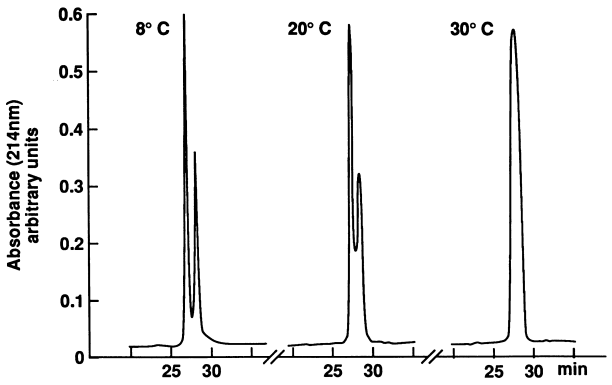

Figure 2 Temperature dependence of the equilibrium isomers of the PRL-R PRM peptide on RP-HPLC

The purified PRL-R PRM peptide was chromatographed on analytical RP-HPLC and eluted with a 0–50% gradient of Buffer B in Buffer A (see the Materials and methods section) over 50 min at 8, 20 and 30 °C.

in different retention times. Secondly, the rate of interconversion between the two conformers must be sufficiently low in relation to the time-scale (min) of the RP-HPLC. Since the rate of proline isomerization should be a function of temperature, the peptide was analysed at temperatures lower (8 °C) and higher (30 °C) than ambient (20 °C) (Figure 2). At 8 °C, the two peaks are almost resolved into two separate peaks. At 20 °C, the region between the two peaks is substantial and is the consequence of conformational inversion during the run resulting in intermediate retention times. At 30 °C , the two peaks coalesce into a single peak. Further increases in temperature would be expected to make this single peak sharper. The more rapid rate of interconversion at 30 °C results in an averaged retention time between that of the two individual conformers.

Addition of flanking residues to the PRM peptide alters the RP-HPLC peak ratios

Two other peptides were synthesized that contained, in addition to the PRM octamer core, flanking residues that occur in the PRL-R cytoplasmic domain [2]. The sequence of PRM4, which contains the four additional contiguous C-terminal residues Lys-Ile-Lys-Gly, is IFPPVPGPKIKG; the sequence of 2PRM4, which contains the PRM4 residues plus the two contiguous N-terminal residues Thr-Cys, is TCIFPPVPGPKIKG. Both PRM4 and 2PRM4 displayed two major peaks when analysed by RP-HPLC at 20 °C (results not shown). However, the peak 1/peak 2 ratio increased as the peptide length was increased as follows: PRM (60:40), PRM4 (70:30), 2PRM4 (80:20). Extending the peptide in either direction from the core PRM octamer appears to stabilize the predominant conformer.

CD spectra of the PRM peptide exhibit temperature dependence

CD was used to characterize the global secondary structure of the PRL-R PRM peptide. Although only eight residues in length, the peptide displays appreciable structure in its far-UV CD spectrum (Figure 3). A single, broad negative extremum is observed which is centred at ~ 215 nm. At 30 °C, the molar ellipticity at the 215 nm minimum was -12200 deg·cm^2·dmol^{-1}. Increasing temperature would be expected to decrease secondary structure and the associated ellipticity by disrupting the stablizing interactions, as in the case of poly(Val-Pro-Gly-Val-Gly), a

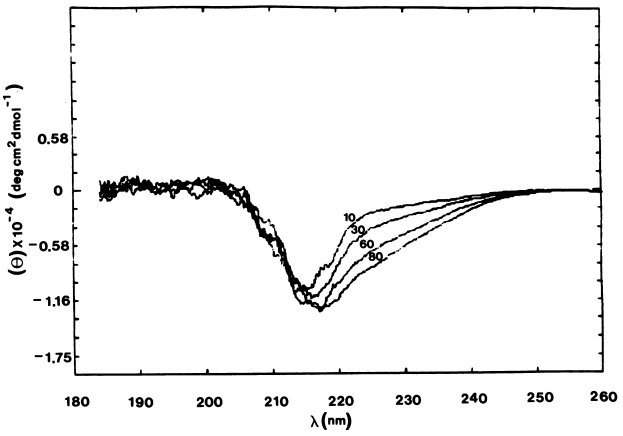

Figure 3 Temperature dependence of CD spectra of the PRL-R PRM peptide

The purified peptide was dissolved at 1 mg/ml in water, pH 2.65. Four temperatures (10, 30, 60 and 80 °C) are shown.

repeating peptide of elastin [45]. In contrast, the spectrum of the PRL-R PRM peptide demonstrates an increase in ellipticity in the 215–245 nm region as the temperature is raised from 10 °C to 80 °C (Figure 3). The temperature effect is most obvious at ~ 225 nm, where the molar ellipticity increases 3.4-fold over the range 10 °C to 80 °C. After cooling the peptide, the original spectra are replicated, demonstrating thermal reversibility of the peptide. An isodichroic point occurs at about 212 nm, which indicates constant ellipticity as a function of temperature and suggests that at least two conformers observable by CD are present and exist in equilibrium. Higher temperatures shift the equilibrium between the conformers. While this spectrum resembles that of a peptide containing β-sheet structure, the absence of any positive peak, particularly in the 200 nm region,

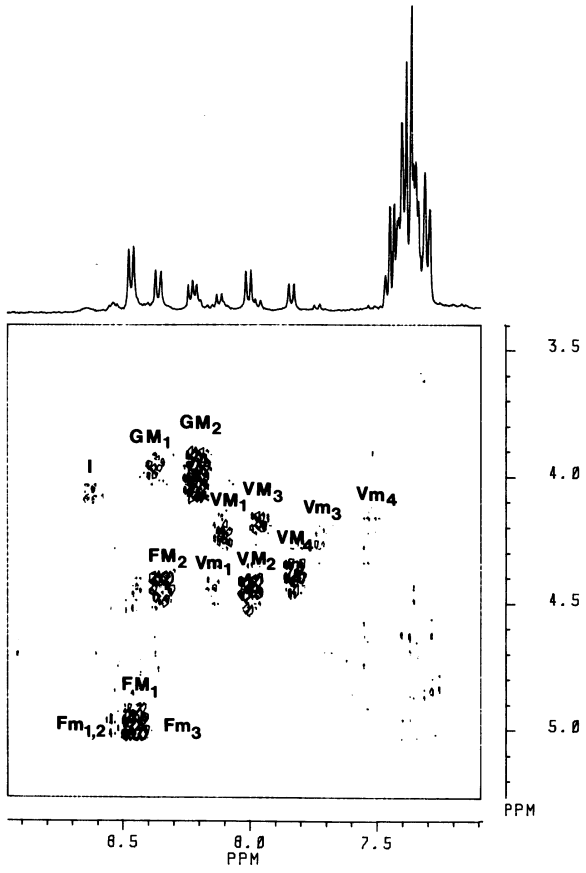

Figure 5 2D-COSY contour plots of the PRL-R PRM peptide

The NH-CαH fingerprint region for the peptide at 40 °C in water is shown. For clarity, the 1D spectrum corresponding to the NH region is also shown. Intense cross-peaks are labelled major (M), while less intense ones are labelled minor (m). FM$_1$, for example, is the first major cross-peak of Phe^2. Some of the minor cross-peaks overlap with major ones as indicated.

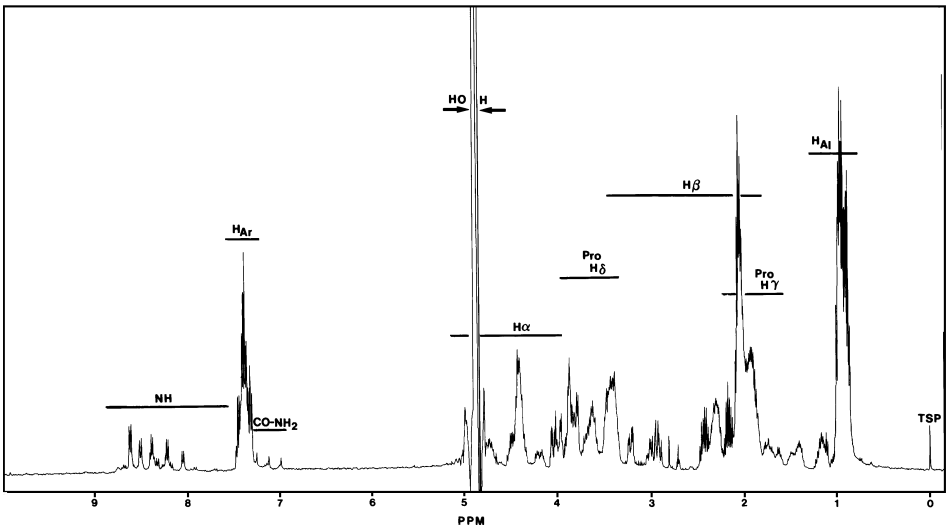

Figure 4 1D ^{1}H-NMR spectrum of the PRL-R PRM peptide

The complete proton spectrum at 25 °C in water is shown. General areas for specific proton types are indicated with bars. NH = amide protons, H_{Ar} = Phe aromatic envelope, CO-NH_2 = terminal ProA, HOH = residual water resonance after suppression, H_{Al} = aliphatic protons from Ile^1 and Val^5 side chains. The spectrum was calibrated against the standard sodium trimethylsilylpropionate.

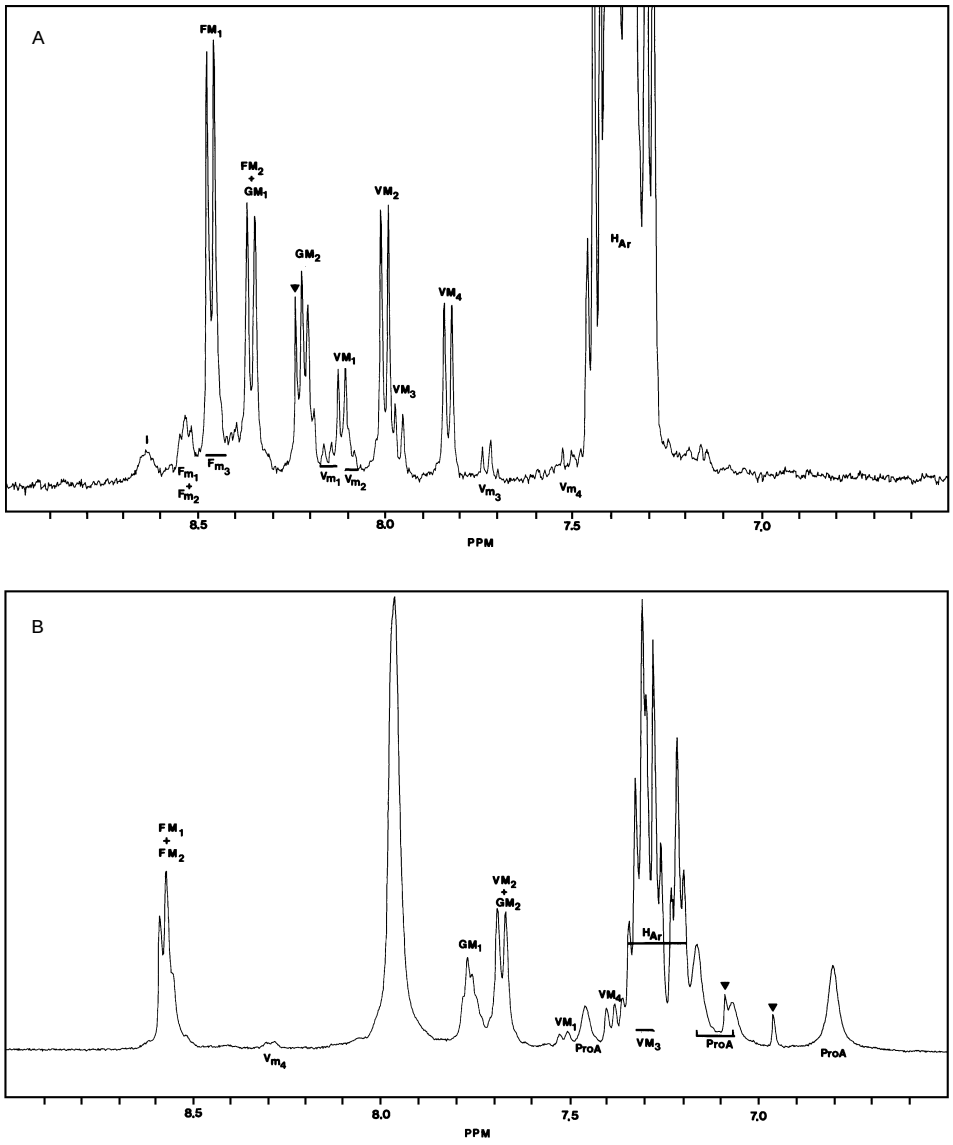

Figure 6 Expansion of the 1D NH region

The amide region of the PRL-R PRM peptide at 40 °C is shown in water (**A**) and DMSO (**B**). Resonances are labelled as in Figure 5. The major resonances are labelled at the top of the peak, while the minor ones are labelled below the peak. Minor signals that are obscured by overlap in these 1D plots are indicated with a bar. The aromatic protons of Phe^2 are also shown (H_{Ar}). At this temperature, the terminal ProA NH_2 protons are not seen in water (**A**) due to rapid exchange, but are visible in DMSO (**B**). Artifacts are indicated by the solid inverted triangles.

suggests that the peptide does not form a β-sheet or β-turn [46,47]. There are no negative ellipticities in the $\sim$ 200 nm range that would be indicative of the polyproline helix [48,49].

To examine the possibility that pH might affect its secondary structure, the peptide was titrated from pH 2.65 to 10.88 in five increments. Only a subtle increase in negative ellipticity at the minimum was noted, without any change in overall spectral shape (results not shown). Acidification of this sample back to pH 4.46 in two steps reversed this minor effect. The single positive charge on the Ile^1 NH_2 group would be neutralized in the higher pH range, resulting in a peptide without any charge. The minor change in the CD spectrum at high pH suggests that this primary amino group does not play a significant role in global structure detectable by this technique. Higher concentrations of peptide ($>$ 1 mg/ml) resulted in a slight red shift of the minimum, suggesting that intermolecular interactions may be significant under these conditions (results not shown).

NMR analysis of the PRM peptide reveals multiple conformers

To determine which proline residue(s) might be giving rise to the two major conformers detectable by RP-HPLC and to study the isomerization of other prolines, 1D- and 2D-^{1}H-NMR studies were performed. The PRL-R PRM peptide was highly soluble in water, even though it contained three hydrophobic amino acids (Ile^1, Phe^2 and Val^5). NMR spectra were acquired at a peptide concentration of 27 mM (22 mg/ml) in water. To characterize the peptide further, comparative studies were also done in DMSO-d_6 at 30 mM (25 mg/ml). As with the CD experiments,

Table 1 Chemical shifts for NH and CαH of the PRL-R PRM peptide at 40 °C in water and DMSO

– indicates resonance not present in DMSO.

		δ (p.p.m.) in water		δ (p.p.m.) in DMSO	
Residue	Resonance	NH	CαH	NH	CαH
Ile^1	I	8.63	4.07	7.97	3.64
Phe^2	Fm_1	8.55	4.98	–	–
	Fm_2	8.53	4.98	–	–
	FM_1	8.46	4.98	8.61	4.72
	Fm_3[a]	8.46	4.47	–	–
	FM_2	8.35	4.42	8.59	4.39
Val^5	Vm_1	8.15	4.21	–	–
VM_1		8.12	4.21	7.72	4.35
Vm_2[b]		8.09	4.21	–	–
VM_2		8.00	4.45	7.55	4.22
VM_3		7.96	4.18[c]	7.43	4.31
VM_4		7.83	4.37	7.27	4.18[c]
Vm_3		7.73	4.28	–	–
Vm_4		7.52	4.17	8.33[e]	4.28
Gly^7	GM_1	8.39[c]	3.99[d]	7.80	3.79, 4.00[f]
	GM_2	8.21	3.99	7.72	3.59, 3.83

[a] Overlaps with FM_1 in 1D spectra; [b] coalescing with VM_1 at 40 °C, completely coalesces at 50 °C, but is resolved at 30 °C; [c] chemical shift identical to that in the random-coil peptide [50]; [d] broad CαH region due to chemical shift overlap; [e] likely to be DMSO analogue of Vm_4 resonance in water based on Δδ; [f] the two Gly CαH protons are resolved in DMSO, but not in water.

25 °C NMR spectra before and after heating to 80 °C were superimposable, indicating that the peptide does not irreversibly denature at high temperatures and peptide concentrations. The complete proton spectrum in water at 25 °C generally shows the expected pattern of resonance lines based on a comparison with the chemical shifts of the same protons in random-coil peptides [50] (Figure 4). Since half of the residues are prolines, the spectrum is dominated by overlapping Pro resonances including Hα (4.3–4.8 p.p.m.), Hδ (3.3–4.0 p.p.m.), Hβ (1.9–2.5 p.p.m.), and Hγ (1.6–2.1 p.p.m.). Since proline lacks an amide proton, the NH region (7.0–9.0 p.p.m.) contains only resonances for Phe^2, Val^5 and Gly^7. In addition, the NH region contains a minor peak corresponding to the N-terminal Ile^1 ammonium group, the Phe^2 aromatic envelope, and several lines corresponding to the C-terminal ProA NH_2 resonances (Figure 4).

Careful inspection of the 1D spectrum of the peptide in water reveals a resonance line pattern that is more complex than would be expected from an 8-amino-acid peptide, but is consistent with the presence of multiple conformers. Proline ring protons have different chemical shifts depending on the *cis* or *trans* conformation of the peptide bond [51]. For example, broad peaks are seen for the two proline ring protons attached to the β-carbon (β_1 and β_2) at 2.0 and 2.3 p.p.m., which are consistent with *trans* Pro [51] (Figure 4). Just downfield from each of these resonances at 2.15 and 2.43 p.p.m. are complex multiplets for the Pro β ring protons in the *cis* conformation [51]. A similar chemical shift dispersion is seen for the Pro δ ring protons. The NH region, which is expanded and assigned in Figure 6, provides the most compelling evidence for multiple isomers since approximately 15 doublets are present instead of the three expected if only one conformer were present. Additional experiments to characterize the structure of the peptide by NOESY were performed, but did not yield contour plots of sufficient intensity, perhaps due to the low nuclear concentrations resulting from multiple conformations.

The 1D ^{1}H-NMR spectrum of the PRL-R PRM peptide in d_6-DMSO (results not shown) is generally similar to that of the peptide in water (Figure 4). However, there are some significant differences. Several regions show a simpler pattern in DMSO than in water, including Pro Hβ (2.0–2.5 p.p.m.), Ile Hγ (1.0–1.5 p.p.m.) and NH regions. The Ile^1 NH_2 group and the C-terminal ProA NH_2 protons gave much more prominent signals in DMSO than in water due to decreased exchange between these protons and the solvent. These observations suggest that hydrogen bonding of water may play an important role in the solvation and stabilization of the peptide.

Analysis of the major amide region resonances

2D-COSY NMR experiments demonstrate through-bond or scalar coupling, which allows resonances to be assigned to the amino acid residues from which they arise. These assignments were made unambiguously for the multiple amide region resonances, providing a basis for understanding proline isomerization in the peptide. 2D-COSY contour plots of the NH-CαH fingerprint region, which demonstrate scalar coupling between amide and alpha protons, of the PRM peptide at 40 °C in water (Figure 5) and DMSO-d_6 (results not shown) are quite similar. Cross-peak assignments are consistent with those in the corresponding expanded 1D NH region spectra (Figures 6A and 6B), with intense peaks designated Major (M) and smaller peaks designated minor (m). The chemical shifts for the NH and CαH protons of the PRL-R PRM peptide in each solvent at 40 °C are provided in Table 1. The assignments were made based on (i) chemical shift values for corresponding residues in random-coil peptides [50], (ii) fine structure of the amide proton resonances, (iii) COSY connectivities of main and side-chain protons, (iv) temperature coefficients of the peaks (Table 2), and (v) consideration of proximal and distal proline isomerization as developed below.

The Phe^2 NH gives rise to two major signals (FM_1 and FM_2) as well as three ill-resolved minor ones ($Fm_{1–3}$) (Figures 5 and 6). Although there are four possible Xaa-Pro bonds in the PRL-R PRM peptide IFPPVPGP (Figure 1), the major Phe^2 NH resonances are likely to be due to local or proximal proline isomerization (i.e. Pro^3), while the minor peaks may be due to distal proline isomerization. Comparison of the FM_1 and FM_2 cross-peaks supports this hypothesis using the following rationale. Since the α proton (CαH) of residue Xaa is closer than the amide proton (NH) to the peptide bond Xaa-Pro by one covalent bond, this α proton is likely to experience a greater change in chemical shift (Δδ) resulting from that proline's isomerization than the amide proton for residue Xaa. Similarly, the amide proton of residue Xaa would show a greater Δδ than the α proton if a proline N-terminal to it were isomerizing (where Yaa-Pro isomerizes in Yaa-Pro-Xaa-Pro). For example, the peptide Ala^1-Tyr^2-Pro^3-Tyr^4-Asp^5-Val^6 demonstrates these chemical shift differences precisely as Pro^3 isomerizes [52]. For Tyr^2, the CαH Δδ is greater (0.40 p.p.m.) than the NH Δδ (0.19 p.p.m.), whereas for Tyr^4, the Δδ of the NH (0.67 p.p.m.) is greater than that of the CαH (0.12 p.p.m.). The FM_1 and FM_2 doublets, which show relatively large differences for the chemical shift of their associated CαHs (0.56 p.p.m. in water), but smaller differences in the NH chemical shifts (0.11 p.p.m.), must be due to local Phe^2-Pro^3 isomerization (Figures 1, 5 and 6A, and Table 1). In DMSO, the major Phe^2 NH resonances are also split by a large CαH Δδ (0.33 p.p.m.), but the NHs are essentially overlapping (Figure 6B, Table 1).

Table 2 Temperature coefficients for amide protons of the PRL-R PRM peptide from 25–40 °C in water and DMSO

– indicates resonance not present or not measurable due to spectral overlap.

Residue	Resonance	Temperature coefficient (−p.p.b./deg) Water	DMSO
Ile[1]	I	7.3	2.0
Phe[2]	Fm_1	10.0	–
	Fm_2	10.0	–
	FM_1	10.0	6.0
	FM_2	10.0	–[a]
Val[5]	VM_1	14.0	8.0
	Vm_2	11.5	–
	VM_2	14.0	9.3
	VM_3	14.0	–[b]
	VM_4	14.0	8.7
	Vm_3	11.3	–
	Vm_4	10.7	8.7
Gly[7]	GM_1	–	8.7
	GM_2	10.7	–

[a] FM_1 overlaps with FM_2 in DMSO; [b] resonance masked by aromatic envelope.

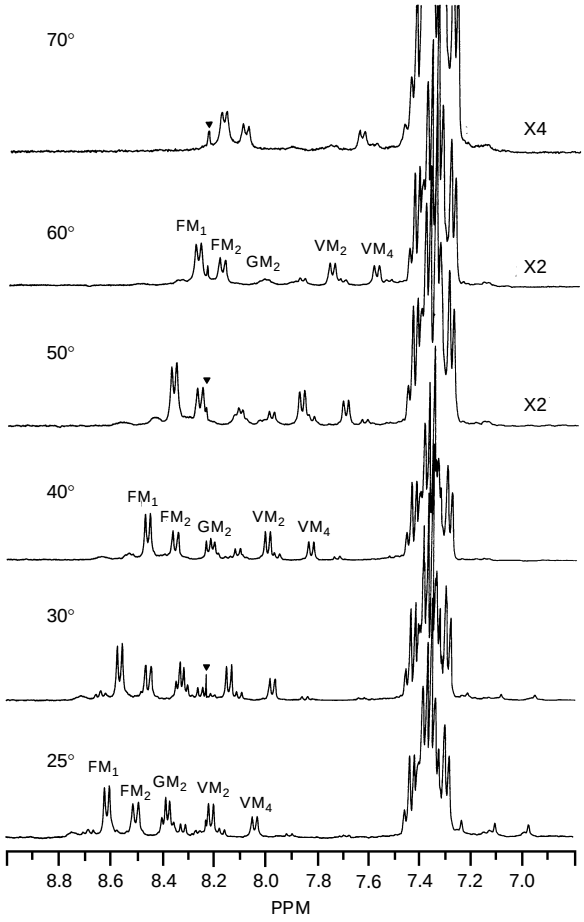

Figure 7 Multi-temperature plot of the 1D NH region of the PRL-R PRM peptide in water

The amide region of the peptide in water is shown at six temperatures (25, 30, 40, 50, 60 and 70 °C). While all of the amide resonances shift upfield with increasing temperature, the large aromatic envelope remains at a constant chemical shift value. The intensity of the signals decreased at higher temperatures due to exchange and were multiplied by the vertical display scale indicated for easier viewing. Some of the major resonances are labelled for orientation (see upper panel of Figure 6 for more detail). The solid inverted triangle marks an artifact with a constant chemical shift value.

The resonance intensity ratio FM_1/FM_2 is $\sim$ 65:35 in water and in DMSO, as determined by peak height comparisons, or by area integrals at higher temperatures. In the case of Phe[2], integration of the two β protons, which are resolved in the 2.95–3.22 region of the spectrum (Figure 4), was also done to confirm the above ratio determinations. Interestingly, the Phe[2] βHs for the conformer reflected by FM_1 showed the expected chemical shifts and splitting pattern (3.22 and 2.95 p.p.m.) [50], while those reflecting the FM_2 conformer were essentially unsplit (3.00 and 3.04 p.p.m.) in water at 25 °C. This unusual pattern for Phe[2] β protons combined with the upfield shift in both the NH and CαH protons associated with FM_2 suggests that this resonance reflects the *cis* isomer of the Phe[2]-Pro[3] bond. The upfield shift of these protons on residues adjacent to a *cis* proline is thought to be due to their close proximity to the anisotropic proline carbonyl group [53]. The predominant resonance, FM_1, represents Pro[3] in *trans* geometry. The *cis*/*trans* ratio for Pro[3] is therefore 35:65 (Table 3).

The Val[5] NH resonance is divided into four major ($VM_{1–4}$) and four minor ($Vm_{1–4}$) signals in water (Figure 6A). The major Val[5] amide peaks are likely to result from the isomerization of the two local prolines (Pro[4] and Pro[6]) adjacent to Val[5]. Inspection of the cross-peaks reveals relatively wide differences in the CαH chemical shifts for VM_1/VM_2 and VM_3/VM_4 ($\sim$ 0.20 p.p.m.), with smaller differences in the chemical shifts for NH (0.12 p.p.m.) in

Table 3 Summary of *cis*/*trans* ratios and relative rates of isomerization of proline in the PRL-R PRM peptide in water and DMSO

The conformers induced by Gly[7]-Pro[8] isomerization in water are not present in DMSO, hence the rate and ratio of Gly[7]-Pro[8] isomerization, though probably occurring, could not be determined as indicated by –.

Proline	Xaa-Pro bond	Isomerization detected? Water	DMSO	*Cis*/*trans* ratios Water	DMSO	Relative rate Water	DMSO
Pro[3]	Phe[2]-Pro[3]	Yes	Yes	35:65	35:65	Intermediate	?[a]
Pro[4]	Pro[3]-Pro[4]	Yes	Yes	40:60	35:65	Slow	Slow
Pro[6]	Val[5]-Pro[6]	Yes	Yes	70:30	70:30	Slow	Intermediate
Pro[8]	Gly[7]-Pro[8]	Yes	No	30:70	–	Fast	–

[a] Unlike the case in water, the major Phe conformers in DMSO actually diverge slightly at higher temperatures making a rate assessment difficult.

water (Figure 5, Table 1). These results suggest VM_1/VM_2, as well as VM_3/VM_4, are related by Val[5]-Pro[6] *cis–trans* isomerization. Comparison of VM_1 and VM_3 yields greater $\Delta\delta$ for NH (0.16 p.p.m.) than for CαH (0.03 p.p.m.). Similar $\Delta\delta$ values between VM_2 and VM_4 are also seen (Table 1). These results indicate that VM_1 is related to VM_3 and VM_2 to VM_4 by Pro[3]-Pro[4] isomerization.

In water, the VM_1/VM_2 and VM_3/VM_4 ratios are 30:70, which reflects Pro[6] isomerization. The ratio of VM_2 to VM_4 and VM_1 to VM_3 due to Pro[4] isomerization is 60:40. Based on the chemical shifts of these four Val[5] resonances and modelling of the peptide to account for the generation of the minor NH resonances (see below), the *cis* or *trans* assignments can be made (Figure 6A, Table 1). Since VM_1 is downfield from VM_2, VM_1 represents Pro[6] in *trans* geometry because *cis* prolines tend to shift protons in the adjacent residue upfield [53]. Similarly, VM_1 and VM_2 are downfield from VM_3 and VM_4, which suggests that Pro[4] is in *trans* for VM_1 and VM_2. To summarize, the major Val[5] peaks of the peptide in water arise from Pro[4] and Pro[6] in the following conformations, respectively: VM_1 (*trans*, *trans*), VM_2 (*trans*, *cis*), VM_3 (*cis*, *trans*), and VM_4 (*cis*, *cis*). In DMSO, the same relationships apply. However, in addition to the upfield shift of the NH resonance going from VM_1 to VM_2, which reflects Pro[6] *trans* $\rightarrow$ *cis*, the corresponding CαHs also shift upfield in DMSO. This effect may reflect differences in solvent hydrophobicity and/or hydrogen bonding. The *cis*/*trans* ratios for each proline, which remain essentially constant over 25–70 °C, are provided in Table 3.

The two cross-peaks for Gly[7] (GM_1 and GM_2, Figure 5) could result from isomerization of the proline on either side (Figure 1). However, the relationship between the NH and CαH chemical shifts of GM_1 and GM_2 in water suggests that the proline N-terminal to Gly[7] (Pro[6]) is responsible for the two conformers since the NH $\Delta\delta$ is large (0.18 p.p.m.) and the CαH chemical shifts are equivalent ($\Delta\delta = 0$ p.p.m.) (Figure 5, Table 1). This interpretation is consistent with the relative rates of Pro[6] versus Pro[8] isomerization, which were revealed by temperature studies described below. The ratio for GM_1/GM_2 is 30:70, the same as that of VM_1/VM_2, in both solvents. While isomerization of the Val[5]-Pro[6] bond gives rise to the two major Gly[7] resonances, the effect of Gly[7]-Pro[8] isomerization is reflected in the minor amide resonances of Phe[2] and Val[5].

Analysis of minor amide region resonances, temperature coefficients and isomerization kinetics

While the major NH resonances result from local or adjacent proline isomerization, the minor NH resonances can be explained by distal proline isomerization. Examination of these minor peaks, three for Phe[2] and four for Val[5], was done over a wide range of temperatures since differential resolution was needed to overcome the problem of spectral overlap (Figure 7). Temperature studies also allow the calculation of temperature coefficients ($\Delta\delta/\Delta T$) (Table 2) and provide a basis for estimating the relative rates of proline isomerization for each of the four prolines in the peptide. In cases where isomerization of the Xaa-Pro bond is relatively rapid, the *cis* and *trans* NH resonances should begin to coalesce with increasing temperature. Completely coalesced peaks at higher temperatures reflect the average chemical shift value for the two conformers on the NMR time-scale. Conversely, peaks arising from slow proline isomerization remain resolved at higher temperatures with a constant chemical shift separation due to the persistence of *cis* and *trans* conformers on the NMR time-scale.

The chemical shift separations between the four major Val[5] NH resonances in water are constant from 25–70 °C. Consistent with this observation, the temperature coefficients for VM_{1-4} in water are all 14.0 (Table 2). At temperatures above 70 °C, all of the amide protons exchange rapidly with the solvent and hence no lines are observed. The separation between VM_1 and VM_2 is constant (0.11 p.p.m.), which suggests slow Pro[6] isomerization; the separation between VM_2 and VM_4 is also constant (0.17 p.p.m.), suggesting slow isomerization for Pro[4] as well. Since the two peaks observed on RP-HPLC must be due to very slow proline isomerization as discussed earlier, either Pro[4] or Pro[6] are reasonable candidates for causing this effect. Temperature studies of the peptide in DMSO reveal that while Pro[4] isomerizes slowly as it also does in water, Pro[6] appears to have faster (intermediate) kinetics in DMSO since the representative resonances begin to coalesce at 25–50 °C (results not shown). Since Pro[4] isomerizes slowly in both solvent systems, this isomerization may generate the two RP-HPLC peaks (Figure 2).

In contrast, Pro[3] appears to isomerize at an intermediate rate in water since the chemical shift separation between FM_1 and FM_2 is constant (0.11 p.p.m.) from 25 to 40 °C, but decreases by 0.01 p.p.m. (coalescing resonances) for each 10 °C increment in the 50–70 °C range. This behaviour suggests an intermediate rate of *cis-trans* isomerization. The rate of isomerization of the remaining proline (Pro[8]) appears to be fast as determined below via an analysis of minor conformers that coalesce in the lower temperature range. This rapid rate of Pro[8] interconversion might be expected because of its terminal location. A summary of the relative isomerization rates for each proline in both solvents is presented in Table 3.

Phe[2] has three minor NH resonances in water (Fm_{1-3}), but none in DMSO (Figures 6A and 6B). Fm_1 and Fm_2 appear together as a triplet, which actually consists of overlapping doublets in the 1D spectrum (Figure 6A). As the temperature is increased from 25 to 60 °C, the Fm_{1-2} triplet completely coalesces into a doublet, indicating it is being affected by a rapid proline isomerization. Since Pro[8] is the only rapidly isomerizing proline, isomerization of this distal Gly[7]-Pro[8] bond must be responsible for the generation and coalescence behaviour of Fm_1 and Fm_2.

Since Pro[8] is not adjacent to Phe[2] in the linear peptide chain, the effect of its rapid isomerization must be occurring through space when the peptide is in a conformation that places these residues in relatively close proximity (Figure 1). A water molecule may be required to bridge this gap since the effects are only noted in water. If Pro[4] and Pro[6] were in *trans* geometry, a structure that would allow the terminal Pro[8] to influence Phe[2] might be favoured. The fraction of the time that the peptide would theoretically adopt this configuration is the product of the respective *trans* ratios for Pro[4] and Pro[6], or $0.60 \times 0.30 = 18\,\%$. Significantly, the peak ratio of $(Fm_1 + Fm_2)/FM_1$ at 30 °C is also $\sim 18\,\%$, which supports this view.

In addition to four major signals, the Val[5] NH gives rise to four minor ones (Vm_{1-4}) in water (Figure 6A). These minor resonances are absent in DMSO except for a single downfield signal, labelled Vm_4 (Figure 6B). Vm_1 and Vm_2 can be understood by examining their coalescence behaviour and their similarity in chemical shift to VM_1. Similar to the temperature-dependent coalescence of Fm_1 and Fm_2, Vm_2 and VM_1 are resolved at 25 °C (8.26 and 8.32 p.p.m.), but partially coalesce at 40 °C (8.09 and 8.12 p.p.m.) and completely coalesce at 50 °C (7.98 p.p.m.). These results suggest that a fast proline isomerization is responsible for the behaviour observed by NMR, which is likely to be due to rapid Pro[8] isomerization. In contrast to Vm_2, Vm_1 does not coalesce with VM_1, but persists at higher temperatures as a shoulder to VM_1. By elimination, Pro[3] must be responsible for this signal. In agreement with this interpretation, the ratio of

VM_1/Vm_1 is similar to that of conformers arising from Pro^3 isomerization (65:35).

DISCUSSION

The biochemical role of the PRM in cytokine receptors

The conservation of the PRM in cytokine receptors [2,3] and the consistent finding that mutations in the PRM disrupt cytokine receptor function [3,25–32] underscore the importance of this short proline-rich sequence. However, the exact molecular role of the PRM is not yet clear. There are several possibilities for the function of the PRM including (i) binding to an SH3 domain, (ii) interacting with a tyrosine kinase such as JAK2, (iii) serving as a site involved in the folding pathway of the cytoplasmic domain to native conformation, or (iv) acting in some other novel capacity. While there is evidence to support a PRM interaction with JAK2, our data suggest a novel function for the PRM. Three lines of evidence suggest that the PRM may not interact with an SH3 domain. SH3 domains, found in many signalling proteins, bind to proline-rich stretches of amino acids in the context of the interacting protein [36–38], although the corresponding peptides bind with relatively low affinity *in vitro* [49,54]. First, the SH3 binding site is different from the PRM. Although prolines in the SH3 binding site consensus sequence Xaa-Pro-Ψ-Pro-Pro-Xaa-Pro (where Ψ represents a hydrophobic amino acid) [54] can be aligned with those in the PRM1 consensus sequence **Al-Ar-Pro$_1$-X-Al-Pro$_2$-X-Pro$_3$** [2], the conserved aliphatic and aromatic residues are not observed. Secondly, the conformation of the PRL-R PRM peptide appears to differ from the conformation of peptides that interact with SH3 domains. NMR solution structures of SH3 domain/peptide complexes indicate that the proline-rich peptides adopt the left-handed polyproline type II (PPII) helix [54]. SH3 domains can recognize proline-containing peptides in both plus (+) and minus (−) orientations [55]. Surprisingly, the presence of proline is not obligatory for the formation of the PPII-helix [19]. Nevertheless, peptides containing PPII-helices have a characteristic far-UV CD spectrum that exhibits an intense negative band at $\sim$ 200 nm [48,49]. The PRL-R PRM peptide does not appear to form a PPII-helix since its CD spectrum lacks this diagnostic minimum at 200 nm, but instead contains a single negative band at $\sim$ 215 nm (Figure 3). At lower temperatures, the CD spectrum of the PRL-R PRM peptide resembles acetamidopyrrolidinone in water, whose negative band in the 210 nm region is attributed to an $n \rightarrow \pi^*$ transition [56]. At higher temperatures, the peptide appears to be in equilibrium with another conformer since the ellipticity increases in the 215–240 nm region, but also has an isodichroic point at $\sim$ 212 nm (Figure 3). The spectral features of this second conformer are similar to those of *N*-acetyl-alanine-*N′*-methylamine, which is believed to form a C_7 γ-turn in non-polar solvents [56]. However, the high temperature coefficients of the PRL-R PRM peptide do not support the presence of an intramolecular hydrogen bond such as is present in the C_7-γ turn (Table 2). The CD spectrum of the peptide is also similar to that of the dipeptide Pro-Pro [57] and the hydrophobic tandemly repeated T-cell epitope peptide H2D8 [48]. The concentration dependence of the CD spectrum suggests that an intermolecular interaction may be occurring (results not shown). Thirdly, the NMR data from the present study indicate that the PRL-R PRM peptide does not adopt a rigid structure like that of a PPII-helix, but instead is very flexible with all four prolines undergoing varying rates of isomerization (Table 3).

Cytokine receptors signal through the activation of the JAK family of tyrosine kinases [4,8,9]. A specific interaction has been demonstrated between the PRL-R and JAK2 [5–7], which has been localized to the membrane-proximal cytoplasmic domain containing the PRM [58]. Since JAK2 has been shown to associate with several cytokine receptors, which all share the conserved PRM, and since deletion or mutation of the membrane-proximal cytoplasmic domain containing the PRM in the PRL-R and GH-R abrogates JAK2 association and activation [58–60], it is reasonable to assume that the PRM mediates the JAK2/receptor interaction. However, the PRL-R deletion construct (Δ243–267) that failed to bind and induce tyrosine phosphorylation of JAK2 contains a relatively large deletion (25 residues), including 17 amino acids in addition to the PRM [58]. A more specific relationship between the GH-R PRM and JAK2 activation is seen in another study where a single proline (Pro^{284}, corresponding to the conserved **Pro$_2$** in the PRM consensus sequence) to alanine mutation disrupts JAK2 phosphorylation and growth signalling [30]. It will be interesting to see if this mutant also prevents JAK2 binding, and whether or not JAK2 binds cytokine receptor tails directly or via adaptor proteins. The fact that JAK2 is also activated in receptors that are not PRM-containing cytokine receptor superfamily members, such as interferon γ receptor [61] and c-*kit* [62], argues against a PRM requirement for interaction with JAK2, although it does not rule out a more general requirement for proline-containing sequences.

Another possible role for the PRM would be to serve as an important site in initiating or regulating protein folding during biosynthesis leading to the native conformation, since proline isomerization is often a rate-determining step in this process [22,63]. In fact this proline isomerization or rearrangement of the conformation of a native protein is thought to be catalysed by the abundant intracellular PPIases, although the exact physiological role of these enzymes remains unknown [64]. Since studies to date of PRM mutants in several cytokine receptors have all shown normal surface expression and binding affinity, the PRM probably does not play a role in the biosynthetic folding reaction.

A fourth and novel idea is that the PRM serves as a binding site for a regulatory PPIase, which together form an 'on–off switch' for cytokine receptor activity [39]. Rotation about a single covalent bond from *cis* to *trans* could alter the conformation of the cytoplasmic domain enabling it to form the requisite subunit dimer or multimer. A possible site is the **Al-Pro$_2$** bond in the PRM consensus sequence. The NMR data on the PRL-R PRM peptide reported here are consistent with this hypothesis. In addition, mutations involving **Pro$_2$**, whether double mutations of **Pro$_2$** and **Pro$_3$** in gp130 [3] and the Nb2 PRL-R [31], or a single mutation of **Pro$_2$** in the GH-R [30] (all of which yield non-functional receptors), also agree with this hypothesis. In this scenario, the PRM would represent the endogenous ligand of the immunophilins that binds to cytokine receptors. Indeed, recent studies have demonstrated an interaction between the immunophilin FKBP12 and a cytokine receptor (transforming growth factor receptor-β) [65], and with two intracellular calcium release channels, the ryanodine receptor [66] and the inositol-1,4,5-triphosphate receptor [67], although a specific binding site remains to be identified. Similarly, the immunophilin that binds to CsA, cyclophilin, appears to be required for the functional expression of homo-oligomeric nicotinic acetycholine receptors [68].

Identification of the proline that generates two RP-HPLC peaks

Synthetic peptides containing Xaa-Pro bonds with exceptionally low rates of isomerization will chromatograph on RP-HPLC as two partially resolved peaks representing the *cis* and *trans* isomers [69–71]. The behaviour of the synthetic peptide Met-Ser-Ile-Pro-Pro-Glu-Lys (MSIPPEK), for example, is essentially identical to

Table 4 Relative abundance of the 16 possible *cis*:*trans* proline configurations of the PRL-R PRM in water

Calculations are based on the multiplication of the relative *cis* or *trans* ratio for each proline (Table 3). Rows highlighted in bold: conformer 1 is the suggested 'active' configuration (all-*trans*), while conformer 4 is the most abundant conformer.

Conformer no.	Pro^3	Pro^4	Pro^6	Pro^8	Total Pro configuration	Percentage of total population (%)
1	***trans***	***trans***	***trans***	***trans***	tttt	8.2
2	*cis*	*trans*	*trans*	*trans*	cttt	4.4
3	*trans*	*cis*	*trans*	*trans*	tctt	5.5
4	***trans***	***trans***	***cis***	***trans***	ttct	19.1
5	*trans*	*trans*	*trans*	*cis*	tttc	3.5
6	*cis*	*cis*	*trans*	*trans*	cctt	2.9
7	*trans*	*cis*	*cis*	*trans*	tcct	12.7
8	*trans*	*trans*	*cis*	*cis*	ttcc	8.2
9	*cis*	*trans*	*cis*	*trans*	ctct	10.3
10	*cis*	*trans*	*trans*	*cis*	cttc	1.9
11	*trans*	*cis*	*trans*	*cis*	tctc	2.3
12	*cis*	*cis*	*cis*	*trans*	ccct	6.9
13	*trans*	*cis*	*cis*	*cis*	tccc	5.5
14	*cis*	*cis*	*trans*	*cis*	cctc	1.3
15	*cis*	*trans*	*cis*	*cis*	ctcc	4.4
16	*cis*	*cis*	*cis*	*cis*	cccc	2.9

that of the PRL-R PRM peptide; both show two partially resolved peaks in equilibrium that coalesce into a single peak at elevated temperatures on RP-HPLC [70] (Figure 2). The authors tentatively assigned the isomerization to the Pro-Pro bond [70]. The Pro^3-Pro^4 bond in the PRL-R PRM peptide is assigned as the site generating the RP-HPLC peaks since it isomerizes slowly in both water and DMSO (Table 3) and a 60:40 conformer ratio is calculated from both NMR and RP-HPLC peak intensities. Additional evidence included the finding that substitution of Pro^4 with Gly in the PRL-R PRM peptide (IFP**G**VPGP, substitution in bold) resulted in a synthetic peptide that chromatographed on RP-HPLC as a single peak at both 10 °C and 25 °C (results not shown).

Since Pro^4 is not conserved in the PRM consensus sequence, it is not likely to be the critical proline in the hypothesis for receptor activation by isomerization although it does produce the RP-HPLC effect. Indeed, the slightly longer peptides PRM4 and 2PRM4 showed decreasing amounts of the second peak on RP-HPLC, suggesting that a full-length cytoplasmic domain would favour a single conformation (*trans*) for this residue.

Hydrogen bonding in the PRL-R PRM peptide in water

Given the amino acid composition of the PRL-R PRM peptide, with three hydrophobic residues and no charged side chains, its high solubility in water is somewhat surprising. Since half of the residues are proline, it is likely that H-bonding of water to the proline carbonyl oxygen plays an important role in solvation. Furthermore, the proton NMR spectra of the PRM peptide are more complex in water than in DMSO. Most of the minor conformers deduced from the amide region of the spectrum of the PRM peptide in water, for example, were not observed in DMSO (Figure 6, Table 1). These results demonstrate an important role for H-bonding in solubilizing and in generating some of the minor conformers of the PRL-R PRM peptide. Intrapeptide hydrogen bonding, however, appears not to occur since the temperature coefficients are relatively high (Table 2), suggesting that the amide protons are solvent exposed. If these residues are similarly exposed in the native PRL-R cytoplasmic domain, they may provide a reasonable binding site for a PPIase [72].

Identification of the biologically relevant proline in the PRL-R PRM peptide

Pro^6 may play an important biological role. It is interesting that Pro^6, which corresponds to the PRM consensus position $\mathbf{Pro_2}$, is the only proline in the PRL-R PRM peptide that favours the *cis* conformation, with a 70:30 ratio (Table 3). Since amino acids that contain bulky side chains and sequentially precede proline appear to favour the *cis* conformation [73], it is not surprising that Val^5-Pro^6 prefers *cis* geometry. The most favourable overall conformation for the peptide is calculated to be *trans-trans-cis-trans* for prolines 3, 4, 6 and 8 respectively. This conformation has an overall relative abundance of 19% (Table 4), and would correspond to the inactive conformation of the receptor in the model. Interestingly, the NMR data suggest that when Pro^6 isomerizes from *cis* to *trans*, the peptide adopts a pseudo-cyclic conformation where Phe^2 and Val^5 are interacting with the terminal Gly^7-Pro^8 residues. This all-*trans* backbone conformation, corresponding to the active conformation of the receptor, can be superimposed on the backbone of the cyclic immunosuppressive drug RAP [23], although the precise three-dimensional structure of the PRL-R PRM peptide is not yet known. Continuing the analogy, an immunophilin such as FKBP may bind to the PRM and regulate this isomerization. It is significant that FK506 also undergoes isomerization from *cis* when in solution to *trans* when bound to FKBP [74]. The *trans* conformer of FK506 has a slightly higher energy, which agrees with the lower abundance of the all-*trans* PRL-R PRM peptide (8%, Table 4). Furthermore, FKBP prefers aliphatic residues in the Xaa position of Xaa-Pro peptide targets, consistent with a conserved aliphatic position in the PRM consensus sequence. It has been suggested that the abundant PPIases may play a direct role in signal transduction by activating an effector protein and then dissociating and allowing the effector protein to slowly revert to its original isomeric state, a process described as setting a 'molecular timer' [75]. Our model supports this idea and extends it by defining a specific binding site for a PPIase such as FKBP (the PRM) acting on a class of proteins (cytokine receptors) as well as suggesting the specific peptide bond (**Al-$\mathbf{Pro_2}$**) on which the enzyme operates. This model is similar to that of Snyder and colleagues [67], which suggests that FKBP can

bind to and regulate the activity of intracellular calcium release channels.

While proline isomerization is recognized as an important process in protein folding to the native state, less is known about isomerization of already folded native proteins. The calcium-binding protein calbindin D_{9K} is a globular protein that has two interconverting proline isomers in its native state as determined by NMR spectroscopy [41]. Mutation of Pro^{43} in calbindin D_{9K} to Gly results in a single conformation [42]. Both *cis* and *trans* conformations for Pro^{43} were also observed in a high-resolution crystal structure of calbindin D_{9K} [76]. In agreement with our findings that local proline isomerization caused the largest $\Delta\delta$ values in the PRL-R PRM peptide, structural changes associated with Pro^{43} isomerization were highly localized in calbindin D_{9K} as determined by NMR and X-ray crystallography. It is not clear whether proline isomerization is involved in the physiological role of calbindin D_{9K}. Proline isomerization was recently observed using NMR in the 22-amino-acid mast cell degranulating (MCD) peptide, although possibly different pharmacological activities of these conformers remains speculative [44].

Summary

The RP-HPLC, CD and NMR studies presented here show that the PRL-R PRM peptide exhibits some unique biochemical characteristics and provide evidence that the PRM may have a novel function in cytokine receptor signalling. Significantly, the PRL-R PRM peptide does not appear to form a PPII-helix, but instead is a very dynamic structure with all prolines undergoing isomerization. Our working hypothesis is that the isomerization of Pro^6 in the peptide, when viewed in the context of the entire receptor, regulates the activity of the receptor like an on-off switch. Although there is no direct link between this model and the available data, the functional importance of the PRM as reported in numerous studies and the conformational data presented in this work are entirely consistent with this isomerization model. The critical proline within the PRM appears to be Pro^6 (**Pro_2** in the consensus sequence) because (i) it is the only absolutely conserved proline in the cytokine receptors [2], (ii) its isomerization leads to a pseudo-cyclic peptide conformation that resembles RAP, and (iii) when mutated it singly disrupts receptor signalling [30].

We envisage that the isomerization of Val^5-Pro^6 is regulated by a PPIase/immunophilin such as FKBP. Direct binding studies between the PRL-R PRM and FKBP12 are in progress. It is possible that the complex of an immunophilin and the PRM of a cytokine receptor then serves as a substrate for binding an effector molecule, as is the case of the interaction between FK506/FKBP and calcineurin for example [77]. Since immunosuppressive drugs like FK506 and RAP are not normally present within cells, the PRM is a reasonable natural or endogenous ligand for the abundant immunophilins.

We thank Dr. Kevin Ballard and Ralph Orkiszewski for performing the MS measurements, and Dr. Tzyy-Chyau Liang for providing the PRM4 and 2PRM4 peptides. The support of Bruker Instruments, Inc. is acknowledged. We are indebted to C.S. Raman for stimulating discussions and Dr. Barry Nall for helpful comments and criticism. This study has been supported by a National Institute of Mental Health M.D./Ph.D. research fellowship F30-MH10343 (K.D.O.), an American Cancer Society grant DK44625 (L.Y.-L.), a NHLBI grant 27341 (J.D.M.), the Keck Center for Computational Biology, and the Texas Children's Hospital Immunology Research Fund (W.T.S.).

REFERENCES

1 Bazan, J. F. (1989) Biochem. Biophys. Res. Commun. **164**, 788–795
2 O'Neal, K. D. and Yu-Lee, L.-Y. (1993) Lymphokine Cytokine Res. **12**, 309–312
3 Murakami, M., Narazaki, M., Hibi, M., Yawata, H., Yasukawa, K., Hamaguchi, M., Taga, T. and Kishimoto, T. (1991) Proc. Natl. Acad. Sci. U.S.A. **88**, 11349–11353
4 Taniguchi, T. (1995) Science **268**, 251–255
5 Rui, H., Kirken, R. A. and Farrar, W. L. (1994) J. Biol. Chem. **269**, 5364–5368
6 Lebrun, J.-J., Ali, S., Sofer, L., Ullrich, A. and Kelly, P. A. (1994) J. Biol. Chem. **269**, 14021–14026
7 Campbell, G. S., Argetsinger, L. S., Ihle, J. N., Kelly, P. A., Rillema, J. A. and Carter-Su, C. (1994) Proc. Natl. Acad. Sci. U.S.A. **91**, 5232–5236
8 Ziemiecki, A., Harpur, A. G. and Wilks, A. F. (1994) Trends Cell Biol. **4**, 207–212
9 Ihle, J. N., Witthuhn, B. A., Quelle, F. W., Yamamoto, K., Thierfelder, W. E., Kreider, B. and Silvennoinen, O. (1994) Trends Biochem. Sci. **19**, 222–227
10 Darnell, J. E., Kerr, I. M. and Stark, G. R. (1994) Science **264**, 1415–1421
11 Elberg, G., Kelly, P. A., Djiane, J., Binder, L. and Gertler, A. (1990) J. Biol. Chem. **265**, 14770–14776
12 Hooper, K. P., Padmanabhan, R. and Ebner, K. E. (1993) J. Biol. Chem. **268**, 22347–22352
13 DeVos, A. M., Ultsch, M. and Kossiakoff, A. A. (1992) Science **255**, 306–312
14 Watowich, S. S., Hilton, D. J. and Lodish, H. F. (1994) Mol. Cell. Biol. **14**, 3535–3549
15 Nakamura, Y., Russell, S. M., Mess, S. A., Friedmann, M., Erdos, M., Francois, C., Jacques, Y., Adelstein, S. and Leonard, W. J. (1994) Nature (London) **369**, 330–333
16 Davis, S., Aldrich, T. H., Stahl, N., Pan, L., Taga, T., Kishimoto, T., Ip, N. Y. and Yancopoulos, G. D. (1993) Science **260**, 1805–1808
17 von Heijne, G. (1991) J. Mol. Biol. **218**, 499–503
18 Wilmot, C. M. and Thornton, J. M. (1988) J. Mol. Biol. **203**, 221–232
19 Adzhubei, A. A. and Sternberg, M. J. E. (1993) J. Mol. Biol. **229**, 472–493
20 MacArthur, M. W. and Thornton, J. M. (1991) J. Mol. Biol. **218**, 397–412
21 Smith, J. A. and Pease, L. G. (1980) CRC Crit. Rev. Biochem. **8**, 315–400
22 Brandts, J. F., Halvorson, H. R. and Brennan, M. (1975) Biochemistry **14**, 4953–4963
23 Schreiber, S. L. (1991) Science **251**, 283–287
24 Sehgal, S. N. and Bansback, C. C. (1993) N. Y. Acad. Sci. **685**, 58–67
25 Sakamaki, K., Miyajima, I., Kitamura, T. and Miyajima, A. (1992) EMBO J. **11**, 3541–3549
26 Fukunaga, R., Ishizaka-Ikeda, E. and Nagata, S. (1993) Cell **74**, 1079–1087
27 Baumann, H., Symes, A. J., Comeau, M. R., Morella, K. K., Wang, Y., Friend, D., Ziegler, S. F., Fink, J. S. and Gearing, D. P. (1994) Mol. Cell. Biol. **14**, 138–146
28 Goldsmith, M. A., Xu, W., Amaral, M. C., Kuczek, E. S. and Greene, W. C. (1994) J. Biol. Chem. **269**, 14698–14704
29 Goujon, L., Allevato, G., Simonin, G., Paquereau, L., Le Cam, A., Clark, J., Nielsen, J. H., Djiane, J., Postel-Vinay, M.-C., Edery, M. and Kelly, P. A. (1994) Proc. Natl. Acad. Sci. U.S.A. **91**, 957–961
30 Wang, Y.-D. and Wood, W. I. (1995) Mol. Endocrinol. **9**, 303–311
31 O'Neal, K. D., Yu-Lee, L.-Y. and Shearer, W. T. (1995) Ann. N. Y. Acad. Sci. **766**, 282–284
32 Takaki, S., Kanazawa, H., Shiiba, M. and Takatsu, K. (1994) Mol. Cell. Biol. **14**, 7404–7413
33 O'Neal, K. D. and Yu-Lee, L.-Y. (1994) J. Biol. Chem. **269**, 26076–26082
34 Ali, S., Edery, M., Pellegrini, I., Lesueur, L., Paly, J., Djiane, J. and Kelly, P. A. (1992) Mol. Endocrinol. **6**, 1242–1248
35 O'Neal, K. D. and Shearer, W. T. (1995) Mol. Cell. Biol. **15**, 4657–4658
36 Cicchetti, P., Mayer, B. J., Theil, G. and Baltimore, D. (1992) Science **257**, 803–806
37 Yu, H., Rosen, M. K., Shin, T. B., Seidel-Dugan, C., Brugge, J. S. and Schreiber, S. L. (1992) Science **258**, 1665–1668
38 Ren, R., Mayer, B. J., Cicchetti, P. and Baltimore, D. (1993) Science **259**, 1157–1161
39 O'Neal, K. D. (1994) Ph.D. Thesis, Baylor College of Medicine
40 Wuthrich, K. (1989) Science **243**, 45–50
41 Chazin, W. J., Kordel, J., Drakenberg, T., Thulin, E., Brodin, P., Grundstrom, T. and Forsen, S. (1989) Proc. Natl. Acad. Sci. U.S.A. **86**, 2195–2198
42 Kordel, J., Forsen, S., Drakenberg, T. and Chazin, W. J. (1990) Biochemistry **29**, 4400–4409
43 Grathwohl, C. and Wuthrich, K. (1981) Biopolymers **20**, 2623–2633
44 Steinmetz, W. E., Bianco, T. I., Zollinger, M. and Pesiri, D. (1994) Peptide Res. **7**, 77–82
45 Arad, O. and Goodman, M. (1990) Biopolymers **29**, 1651–1668
46 Johnson, W. C., Jr. (1990) Prot. Struct. Funct. Gen. **7**, 205–214
47 Brahmachari, S. K., Rapaka, R. S., Bhatnagar, R. S. and Ananthanarayanan, V. S. (1982) Biopolymers **21**, 1107–1125
48 Fontenot, J. D., Finn, O. J., Dales, N., Andrews, P. C. and Montelaro, R. C. (1993) Peptide Res. **6**, 330–336
49 Viguera, A. R., Arrondo, J. L. R., Musacchio, A., Saraste, M. and Serrano, L. (1994) Biochemistry **33**, 10925–10933
50 Wuthrich, K. (1986) in NMR of Proteins and Nucleic Acids, John Wiley & Sons, New York

51 Pogliani, L., Ellenberger, M., Valat, J. and Bellocq, A. M. (1975) Int. J. Peptide Protein Res. **7**, 345–360
52 Dyson, H. J., Rance, M., Houghten, R. A., Lerner, R. A. and Wright, P. E. (1988) J. Mol. Biol. **201**, 161–200
53 Poznanski, J., Ejchart, A., Wierzchowshi, K. L. and Ciurak, M. (1993) Biopolymers **33**, 781–795
54 Yu, H., Chen, J. K., Feng, S., Dalgarno, D. C., Brauer, A. W. and Schreiber, S. L. (1994) Cell **76**, 933–945
55 Lim, W. A., Richards, F. M. and Fox, R. O. (1994) Nature (London) **372**, 375–379
56 Madison, V. and Kopple, K. D. (1980) J. Am. Chem. Soc. **102**, 4855–4863
57 Madison, V. and Schellman, J. (1970) Biopolymers **9**, 511–567
58 Lebrun, J.-J., Ali, S., Ullrich, A. and Kelly, P. A. (1995) J. Biol. Chem. **270**, 10664–10670
59 Vanderkuur, J. A., Wang, X., Zhang, L., Campbell, G. S., Allevato, G., Billestrup, N., Norsedt, G. and Carter-Su, C. (1994) J. Biol. Chem. **269**, 21709–21717
60 Frank, S. J., Gilliland, G., Kraft, A. S. and Arnold, C. S. (1994) Endocrinology **135**, 2228–2239
61 Watling, D., Guschin, D., Muller, M., Silvennoinen, O., Witthuhn, B. A., Quelle, F. W., Rogers, N. C., Schindler, C., Stark, G. R., Ihle, J. N. and Kerr, I. M. (1993) Nature (London) **366**, 166–170
62 Brizzi, M. F., Zini, M. G., Aronica, M. G., Blechman, J. M., Yarden, Y. and Pegoraro, L. (1994) J. Biol. Chem. **269**, 31680–31684
63 Mucke, M. and Schmid, F. X. (1994) Biochemistry **33**, 14608–14619
64 Gething, M.-J. and Sambrook, J. (1992) Nature (London) **355**, 33–45
65 Wang, T., Donahoe, P. K. and Zervos, A. S. (1994) Science **265**, 674–676
66 Brillantes, A.-M. B., Ondrias, K., Scott, A., Kobrinsky, E., Ondriasova, E., Moschella, M. C., Jayaraman, T., Landers, M., Ehrlich, B. E. and Marks, A. R. (1994) Cell **77**, 513–523
67 Cameron, A. M., Steiner, J. P., Sabatini, D. M., Kaplin, A. I., Walensky, L. D. and Snyder, S. H. (1995) Proc. Natl. Acad. Sci. U.S.A. **92**, 1784–1788
68 Helekar, S. A., Char, D., Neff, S. and Patrick, J. (1994) Neuron **12**, 179–189
69 Melander, W. R., Jacobson, J. and Horvath, C. (1982) J. Chromatogr. **234**, 269–276
70 Gesquiere, J. C., Diesis, E., Cung, M. T. and Tartar, A. (1989) J. Chromatogr. **478**, 121–129
71 Henderson, D. E. and Mello, J. A. (1990) J. Chromatogr. **499**, 79–88
72 Veeraraghavan, S. and Nall, B. T. (1994) Biochemistry **33**, 687–692
73 Harrison, R. K. and Stein, R. L. (1990) Biochemistry **29**, 1684–1689
74 Van Duyne, G. D., Standaert, R. F., Karplus, P. A., Schreiber, S. L. and Clardy, J. (1991) Science **252**, 839–842
75 Schmid, F. X., Lang, K., Kiefhaber, T., Mayer, S. and Schonbrunner, E. R. (1991) in Conformations and Forces in Protein Folding (Nall, B. T. and Dill, K. A., eds.), pp. 198–203, American Association for the Advancement of Science, Washington, D. C.
76 Svensson, L. A., Thulin, E. and Forsen, S. (1992) J. Mol. Biol. **223**, 601–606
77 Schreiber, S. L. (1992) Cell **70**, 365–368

Received 17 August 1995/7 December 1995; accepted 15 December 1995